Hydrogeochemical Characteristics of the Geothermal System in the Woka-Cuona Rift Zone, Tibet

Wen Zhang *, Jiansong Peng *, Yong Liu

Posted Date: 12 January 2024

doi: 10.20944/preprints202401.0953.v1

Keywords: geothermal system; hydrochemistry; isotope; Woka-Cuona rift

Article

Hydrogeochemical Characteristics of the Geothermal System in the Woka-Cuona Rift Zone, Tibet

Wen Zhang [1,*], Jiansong Peng [2,*] and Yong Liu [1]

[1] Institute of Exploration Technology, Chinese Academy of Geological Sciences, Chengdu 611734, China; 1039786137@qq.com
[2] College of Management Science, Chengdu University of Technology, Chengdu 610051. China
* Correspondence: 3463287@qq.com (W.Z.); 1341227608@qq.com (J.P.)

Abstract: The Woka-Cuona rift zone, situated in the easternmost portion of southern Tibet, displays complex geological conditions. It consists of three distinct grabens or half grabens, spanning the Himalayan and Gangdese terranes from south to north. Examining the distribution patterns and genetic mechanism of the geothermal system in the Woka-Cuona rift zone holds significant guidance for studying the genetic mechanisms of geothermal systems and the production and utilization of geothermal resources in the rift zones of southern Tibet. Based on the geological conditions of the study area, the mechanism of rift formation and the distribution characteristics of geothermal water in the three distinct grabens were analyzed through data collection, ground surveys, geochemical analysis, and isotope analysis. Alongside topographic, drainage, and structural features, the Woka-Cuona rift zone was subdivided into four zones from north to south - Woka, Qiongduojiang, northern Cuona, and southern Cuona grabens. Additionally, the study investigated the geochemical characteristics, recharge sources, and water-rock interactions of geothermal water in different zones, providing a scientific foundation for subsequent geothermal energy production.

Keywords: geothermal system; hydrochemistry; isotope; Woka-Cuona rift

1. Introduction

From the late 1960s to the early 1970s, geothermal energy garnered considerable global attention amidst the oil crisis. China, with the most substantial geothermal activity, possesses potential geothermal reserves constituting 7.9% of the global total. These reserves, however, exhibit uneven distribution influenced by various factors [1–3]. The exploration and assessment of China's geothermal resources have progressively attracted the interest of scientists both domestically and internationally.

Regarding the origin of geothermal water, White [4] proposed a classic genetic mode. Under the conditions of high terrestrial heat flow, meteoric water infiltrates downward through fracture zones or long, deep fissures. Driven by head pressure, it flows across surrounding rocks or deep heat sources, resulting in the formation of geothermal water due to the heating. Ultimately, it ascends to the surface along dominant structural positions, guided by thermodynamic effects. This intricate process involves a continuous exchange of matter and energy between infiltrating rainwater and the subsurface environment, leading to alterations in hydrogeochemical characteristics. Hence, hydrogeochemical characteristics play a crucial role in analyzing the circulation, water-rock interaction, runoff path, and accumulation environment of groundwater.

Hydrochemical and isotopic geochemical characteristics play a significant role in elucidating the genetic mechanism of geothermal water. Since the 1950s, isotope hydrology has been employed in hydrogeological research to unveil the origin, occurrence, distribution, migration, and circulation modes of water in the hydrosphere, as well as its interaction with other Earth spheres [5–7]. Focusing on the geothermal system in the Woka-Cuona rift zone, this study identified the distribution of geothermal water by systematically summarizing the geological settings, structures, and

 doi:10.20944/preprints202401.0953.v1

hydrogeological conditions of the rift zone. Additionally, it examined the hydrogeochemical characteristics of geothermal water through hydrochemical and isotopic analysis methods. The primary goal of this study is to offer robust support for the scientific production of geothermal resources by gaining a deep understanding of the formation mechanism of the geothermal system in the Woka-Cuona rift zone.

2. Overview of the Study Area

The study area, located in southern Tibet, exhibits distinctive topographical features with elevated southern and western sections and lower northern and eastern sections, boasting an average elevation of approximately 5000 m. The Yarlung Zangbo River traverses the area from west to east. The northern portion experiences a plateau temperate subhumid climate, while the southern border area has a plateau subtropical humid climate, characterized by well-defined rainy and dry seasons, with the rainy period lasting from July to September. Additionally, the area receives an average annual precipitation of 300–450 mm and maintains an average annual temperature of around 6℃.

The exposed strata in the study area are predominantly Mesozoic, followed by some Paleozoic and Quaternary strata. The oldest exposed Precambrian strata, including the Duizala Formation (Pt_1y), the Nyalam Group ($Pt_{1-2}Nl$), and the Qudegong Formation (Pt_3Cq), consist of metamorphic core complexes. The Mesozoic strata, comprising the Nieru (T_3n), Qulonggongba ($T_{2-3}q$), Ridang (J_1r), Lure ($J_{1-2}l$), Jiabula (Kj), and Zongzhuo (K_3z) formations, are characterized by sandstones, siltstones, and slates. The Quaternary strata primarily consist of alluvial (Q^{hal}) and proluvial (Q^{hpl}) deposits.

Moving from south to north, the study area features two major first-order faults (Figure 1): the southern Tibetan detachment system and the Yarlung Zangbo suture zone. These are followed by second-order faults, including the Maizhokunggar-Gongbo'gyamda, Zhegucuo-Longzi, and Quzhuomu-Juela faults. Notably, the southern Tibetan detachment system and the Maizhokunggar-Gongbo'gyamda fault control the southern and northern boundaries of the geothermal water exposed in the study area.

Preprints.org (www.preprints.org) | NOT PEER-REVIEWED | Posted: 12 January 2024 doi:10.20944/preprints202401.0953.v1

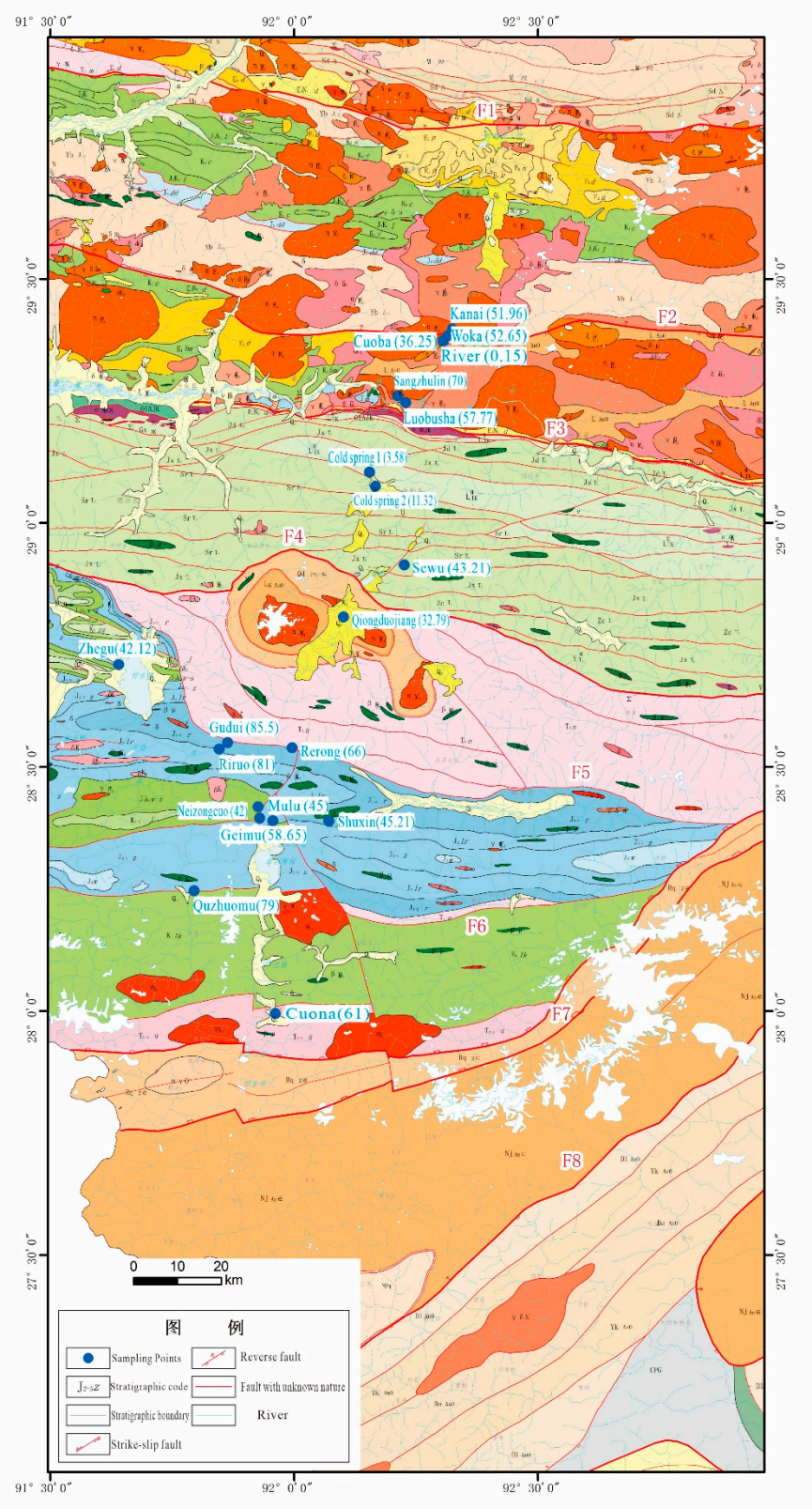

Figure 1. Geologic sketch map of the study area.

According to the classification criteria for aquifer media and groundwater dynamic characteristics, the groundwater in the study area can be categorized into unconsolidated rock pore water and bedrock (clastic and intrusive rocks) fissure water. The former, primarily recharged by river water, is predominantly found in sandy gravel layers dominated by sandstones in the Quaternary terraces along basins and river valleys. The latter, mainly recharged by meteoric water

 doi:10.20944/preprints202401.0953.v1

and characterized by relatively low water content, is primarily present as confined water in the fissures of clastic and intrusive rocks, with granites being the dominant lithotype.

The field survey and collected data indicate the presence of 16 geothermal water sites or geothermal fields spreading across the Woka-Cuona rift zone. Utilizing the distribution and temperature indications of geothermal water, river basin characteristics, and regional structural characteristics, geothermal water in the Woka-Cuona rift zone was categorized into three parts: geothermal water in the Woka, Qiongduojiang, and Cuona grabens.

3. Materials and Methods

Based on geological surveys, this study collected geothermal water samples from the Woka-Cuona rift zone during the period from December 2019 to February 2020. The analysis of these geothermal water samples included field testing, total analysis, and hydrogen, oxygen, and carbon isotope analyses. As a point of comparison, geothermal water from Zhegu outside the grabens was sampled as contrast samples. Additionally, river and cold-spring water within the rift zone was sampled for comparative analysis as background factors.

For on-site water quality analysis, this study utilized an American SMARTROLL handheld multi-parameter water quality monitor as a portable water quality analyzer. The total analysis of the samples was performed by Sino Shaanxi Nuclear Industry Group Comprehensive Analysis and Testing Co., Ltd. The water samples were stored in polyethylene bottles. In the case of polyethylene bottles with a volume of 600 mL, the same water samples would be stored in two bottles, with one sample mixed with 5 ml of a 1:1 nitric acid solution.

Polyethylene bottles with a volume of 50 mL were used to store samples for hydrogen and oxygen isotope analysis. These bottles were initially rinsed three times with water to be sampled before filling to avoid air bubbles. Hydrogen and oxygen isotopes were determined using a MAT-253 stable isotope ratio mass spectrometer, with a precision level better than 0.05%. Additionally, samples for $\delta^{13}C$ dating were stored in polyethylene bottles with a volume of 50 mL, containing 1‰ of saturated $HgCl_2$ solution. The $\delta^{13}C$ was determined using a MAT-253 stable isotope ratio mass spectrometer and a Gas Bench II universal online gas preparation and introduction system, with an absolute error below 0.15‰. All testing procedures were performed by the Karst Geological Resources and Environment Supervision and Testing Center, Ministry of Natural Resources.

4. Results

4.1. Major Elements

To comprehensively understand the genetic mechanism of the geothermal water system throughout the entire rift zone, this study elucidated the physicochemical parameters and major-element characteristics of geothermal, cold-spring, and surface waters. The Woka-Cuona rift zone was divided into the Woka, Qiongduojiang, northern Cuona, and southern Cuona grabens, and Piper diagrams were generated to describe the hydrochemical characteristics, as illustrated in Figure 2.

 doi:10.20944/preprints202401.0953.v1

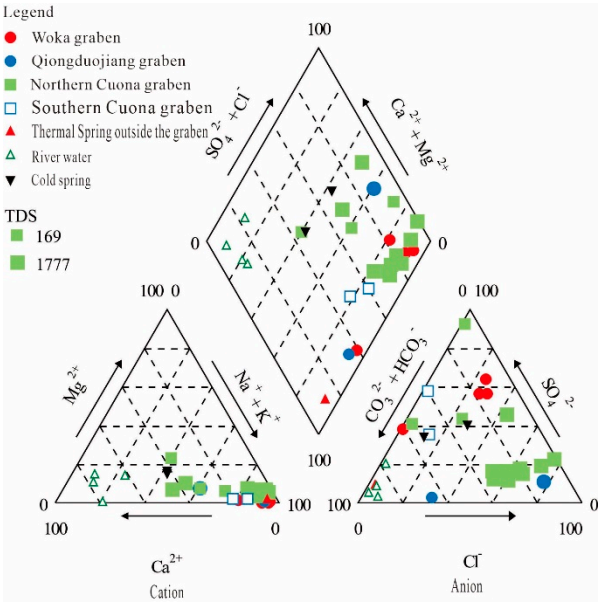

Figure 2. Water chemistry piper diagram.

According to the calculated results, geothermal water samples from the study area contained major cations represented by Na^+ and K^+, followed by Ca^{2+} and Mg^{2+}, while major anions included Cl^-, succeeded by HCO_3^- and SO_4^{2-}. Notably, Na^+, K^+, and Cl^- were identified as critical ions determining the total dissolved solids (TDS) content of the geothermal water samples. In the Woka graben, Na^+ and SO_4^{2-} were predominant in the geothermal water samples. The hydrochemical types of sampling sites Sewu and Qiuduojiang in the Qiongduojiang graben were identified as HCO_3·Cl-Na and Cl-Na·Ca types, respectively, indicating different sources of hydrothermal resources. The geothermal water samples from the northern Cuona graben displayed major cations of Na^+, followed by Ca^{2+}, K^+, and Mg^{2+}, along with major anions of Cl^-, succeeded by HCO_3^- and SO_4^{2-}, suggesting diverse hydrochemical types. Surface and borehole water samples from Cuona in the southern Cuona graben were classified as SO_4·HCO_3-Na and HCO_3·SO_4-Na types, respectively. Geothermal water sampled outside the grabens exhibited the HCO_3·SO_4-Na type.

(1) Woka graben

Geothermal water samples from the Woka graben exhibited temperatures ranging from 36 to 70 ℃ (average: 54℃), pH values falling between 7.95 and 9.25 (average: 8.43; predominantly neutral to slightly alkaline), and TDS contents varying from 120 to 327 mg/L (average: 248.25 mg/L). Various hydrochemical types were observed within the graben, with the SO_4·Cl-Na type predominant in Kanai, Woka, and Cuoba, and the HCO_3·SO_4-Na type in Sangzhuling. In terms of hydrochemical types, the prevalent cation and anion in the geothermal water of the Woka graben are Na^+ and SO_4^{2-}, respectively.

(2) Qiongduojiang graben

Geothermal water samples from Sewu and Qiuduojiang within the Qiongduojiang graben displayed different hydrochemical indicators. Sewu has a pH of 7.67, while Qiuduojiang has a pH of 6.69. The HCO_3^- concentrations are slightly different, with 177 mg/L for Sewu and 189 mg/L for Qiuduojiang, and temperatures of 43℃ and 33℃, respectively. Additionally, the concentrations of Na^+, K^+, Ca^{2+}, Mg^{2+}, Cl^-, and SO_4^{2-} in the geothermal water of Qiuduojiang were considerably higher than those in the geothermal water of Sewu. Hydrochemical types for Sewu and Qiuduojiang were identified as HCO_3·Cl-Na and Cl-Na·Ca types, respectively.

(3) Northern Cuona graben

Geothermal water samples from the northern Cuona graben exhibited temperatures ranging from 42 to 85.5 ℃ (average: 76 ℃), pH values falling between 6.34 and 8.67 (average: 7.54; predominantly neutral to slightly alkaline), and TDS contents varying from 169 to 1777 mg/L (average: 1198 mg/L). On average, these samples contained major cations of Na^+ and Ca^{2+}, followed by K^+ and Mg^{2+}, and major anions of Cl^-, followed by HCO_3^- and SO_4^{2-}. Specifically, the geothermal

 doi:10.20944/preprints202401.0953.v1

water from the ZK251 borehole displayed a temperature of up to 163℃ and TDS content of 1777 mg/L, with higher concentrations of Na^+, K^+, Cl^-, and TDS content compared to other geothermal water in the graben. Conversely, the geothermal water from Geimu showed a minimum TDS value of 169 mg/L, suggesting significant mixing with low-TDS-content cold water.

(4) Southern Cuona graben

Geothermal water samples from two sites in the southern Cuona graben presented slightly different hydrochemical indicators, with temperatures of 56℃ and 55℃, pH values of 8.83 and 8.93, and TDS contents of 240 mg/L and 175 mg/L, respectively. In comparison to water from a borehole drilled in Cuona, spring water from Cuona exhibited higher concentrations of Na^+, K^+, HCO_3^-, and SO_4^{2-}, lower concentrations of Ca^{2+} and Cl^-, and equal concentrations of Mg^{2+}. The geothermal water from the southern Cuona graben showed lower conventional ion contents compared to that from the northern Cuona graben. The hydrochemical types of geothermal water in the Cuona graben were identified as SO_4·HCO_3-Na and HCO_3·SO_4-Na types.

(5) Geothermal water outside the grabens

Geothermal water outside the grabens was exclusively sampled from Zhegu, revealing a temperature of 42℃, a nearly neutral pH value of 7.45, Na^+-dominant cations, and HCO_3^--dominant anions. Its TDS content was 401 mg/L, higher than that of geothermal water from the southern Cuona graben and cold-spring water, but lower than the average TDS contents of geothermal water from the Woka, Qiongduojiang, and northern Cuona grabens. The geothermal water outside the grabens was categorized as the HCO_3·SO_4-Na type.

(6) Cold-spring water

Cold-spring water was solely sampled from the Woka graben and the south side of the Yarlung Zangbo suture zone. Water samples from Nos. 1 and 2 cold springs exhibited temperatures of 4℃ and 11℃, pH values of 7.73 and 7.35, and TDS contents of 365 mg/L and 173 mg/L, respectively. The water samples from the No. 1 cold spring had higher concentrations of conventional ions compared to those from the No. 2 cold spring. The hydrochemical types of the two cold springs were identified as SO_4·Cl·HCO_3-Ca·Na and HCO_3·SO_4-Ca·Na types, respectively, without any significant dominant ions.

(7) River water

River water samples displayed temperatures ranging from 4 to 11℃ (average: 7℃), pH values between 7.76 and 9.65 (average: 8.38; slightly alkaline), and TDS contents ranging from 13 to 85 mg/L, with an average of 56 mg/L, considerably lower than those of geothermal and cold-spring water samples. Cation and anion concentrations ranked as follows: Ca^2>Na^+>Mg^{2+}>K^+ and HCO_3^->SO_4^{2-}>Cl^-. Their dominant anions and cations were notably distinct from those in geothermal and cold-spring water samples. The hydrochemical types of river water samples were identified as HCO_3-Ca·Na for Zengqiqu and HCO_3-Ca for Jiaboxiongqu, Qienaqu, and Cuonaqu.

4.2. Isotopic Characteristics

(1) Hydrogen and oxygen isotopes

Geothermal water samples from the study area exhibited δD values (Table 1) ranging from -161‰ to -128‰ (average: -147‰) and $\delta^{18}O$ values varying from -20.2‰ to -12.0‰ (average: -17.7‰). Water samples from the Nos. 1 and 2 cold springs displayed δD values of -132.0‰ and -142‰ and $\delta^{18}O$ values of -17.0‰ and -17.8‰, respectively. River water samples showed δD and $\delta^{18}O$ values of -146‰ and -18.8‰, respectively.

Table 1. Isotope composition (δD and δ18O) and d values of sampling points in the study area.

Location	Thermal Spring	δD/‰	$\delta^{18}O$/‰	Elevation /m	Reference Value /‰	d Value /‰
Woka graben	Kanai	-156	-19.9	3933	-126	2.6
	Cuo Ba	-151	-19.5	3988	-126	4.9
	Woka	-155	-19.7	3920	-126	2.9

 doi:10.20944/preprints202401.0953.v1

Qiongduojiang graben	Sewu	-155	-20.0	4400	-126	5.1
	Qiongduojiang	-147	-18.1	4440	-126	-2.1
Geothermal water outside the grabens	Zhegu	-161	-19.8	4600	-126	-2.9
Northern Cuona graben	Riruo	-143	-16.4	4440	-126	-11.2
	Re Rong	-145	-17.7	4248	-126	-3.4
	GuDui Q003	-143	-16.4	4388	-126	-11.8
	GuDui Q006	-140	-15.5	4388	-126	-16.0
	GuDui Q007	-143	-16.3	4388	-126	-12.6
	GuDui Q012	-143	-15.8	4388	-126	-16.6
	GuDui Q010	-142	-15.8	4388	-126	-15.6
	GuDui ZK251	-139	-15.5	/	-126	-15.0
	Neizong Cuo	-157	-20.2	5020	-126	4.4
	Geimu	-149	-19.4	4950	-126	5.6
	Mulu	-145	-17.5	4700	-126	-5.7
	Shuxin	-150	-19.0	4320	-126	2.2
	Qu Zhuo Mu	-128	-15.8	4360	-126	-1.9
	Maximum Value	-128	-12.0	5020	-126	5.6
	Minimum Value	-161	-20.2	3568	-126	-33.8
	Average Value	-147	-17.7	4317	-126	-5.4
Zengqiqu	River Water	-146	-18.8	4028	-126	4.3
Cold-spring water	Cold spring 1	-132	-17.0	3954	-126	4.4
	Cold spring 2	-142	-17.8	3875	-126	0.5

(2) Carbon isotopes

Geothermal water samples from the study area exhibited $\delta^{13}C$ values between -7.3‰ and 2.5‰, averaging -2.5‰. Within the Woka graben, geothermal water samples showed $\delta^{13}C$ values ranging from -6.5‰ to -3.5‰, with an average of -5.4‰. Despite both Sewu and Qiuduojiang being in the Qiongduojiang graben, their geothermal water exhibited significantly different $\delta^{13}C$ values of -7.3‰ and 0.5‰, indicating distinct carbon sources. The northern Cuona graben's geothermal water samples showed $\delta^{13}C$ values ranging from -1.5‰ to 2.5‰ (average: 0‰), whereas Cuona's samples displayed relatively constant $\delta^{13}C$ values, suggesting a shared source. The geothermal water sample of Zhegu, located outside the grabens, exhibited a $\delta^{13}C$ value of -4‰, and the river water samples from Zengqiqu yielded a $\delta^{13}C$ value of -7.4‰.

5. Discussion

5.1. Recharge Source and Elevation of Geothermal Water

Due to the inherent presence of deuterium (D) and oxygen (O) as components of water, they offer a natural advantage in tracing the water source (Ren et al., 2022). Craig [8] initially proposed a global meteoric water line (Equation. 1), widely employed for identifying water sources. Zheng SH et al. [9] established China's meteoric water line (Equation. 2). Ning AF et al. [10] obtained a meteoric water line for the Lhasa River region based on the δD and $\delta^{18}O$ values from 21 sets of rainwater samples (Equation. 3), also testing the δD and $\delta^{18}O$ values of rainwater from various years monitored at the Lhasa rainfall monitoring station.

$$\delta D=8\times\delta^{18}O+10 \quad (1)$$

 doi:10.20944/preprints202401.0953.v1

$$\delta D=7.9\times\delta^{18}O+8.2 \quad (2)$$

$$\delta D=7.2\times\delta^{18}O+12.36 \quad (3)$$

Generally, the δD and $\delta^{18}O$ values of geothermal water typically deviate from meteoric water lines [11]. As illustrated in Figure 3a, the δD and $\delta^{18}O$ values of geothermal water from all sampling sites in the study area fall to the right of the global, China's, and Lhasa River region's meteoric water lines. They are distributed along the evaporation line (Figure 3b), indicating that the recharge source of geothermal water at the sampling sites in the study area predominantly originates from meteoric water. However, all geothermal water samples exhibited lower δD and $\delta^{18}O$ values compared to Lhasa's rainwater samples [11], suggesting that the recharge source is likely meltwater formed from meteoric water at higher elevations. If cold-spring and river water in the study area had solely received recharge from meteoric water, their δD and $\delta^{18}O$ values would be close to those of rainwater or higher due to evaporation. However, they exhibited lower δD and $\delta^{18}O$ values compared to the rainwater monitored at the Lhasa rainwater monitoring station. This suggests that they also received recharge from snowmelt at higher elevations, which subsequently mixed with local meteoric water.

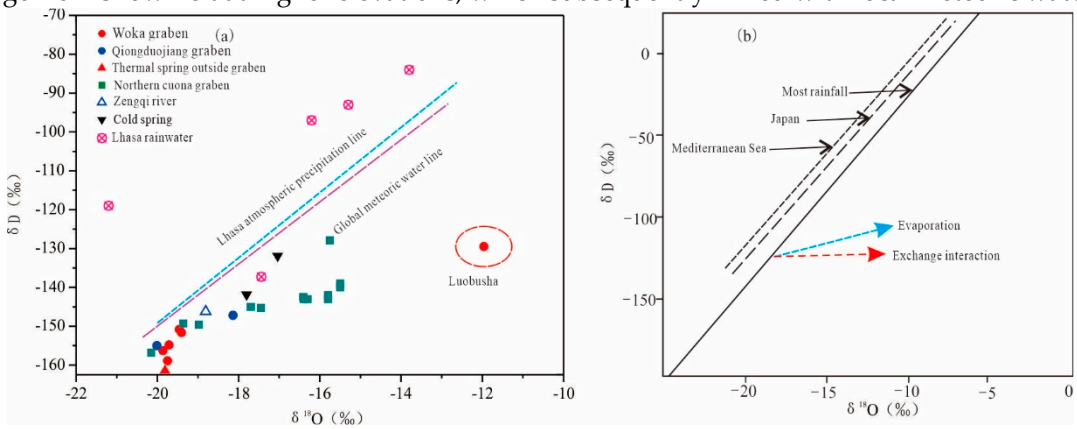

Figure 3. D-O relationship of sampling points in the study area (Figure b modified from [11]).

Considering that Cl^- is relatively stable and not easily adsorbed, it can be effectively used to examine the recharge source and evolution of geothermal water, particularly when combined with the end-element mixing model for stable isotopes [5]. Figure 4 illustrates the δD versus Cl^- (a) and $\delta^{18}O$ versus Cl^- (b) relationships of geothermal water from the sampling sites in the study area. Overall, the δD and $\delta^{18}O$ values of geothermal water exhibited an increase with rising Cl^- concentrations. A positive correlation was observed between Cl^- and water temperature, and the characteristic components of groundwater also showed an increase with higher Cl^- concentrations. This suggests that the participation of Cl^-, F, H_2SiO_3, Li, and B, and the enrichment of $\delta^{18}O$ in geothermal water originate from the same process. In this process, meltwater likely recharged groundwater along fissure and fracture zones, accompanied by the involvement of thermal fluids enriched in Cl^-, F, H_2SiO_3, Li, B, and heavy isotopes at different depths. This led to more substantial water-rock interactions and higher geothermal reservoir temperatures. Geothermal water in the Woka and Cuona grabens exhibited low concentration, as illustrated in Figures 5a and 6, indicating that they belong to distinct geothermal water systems.

 doi:10.20944/preprints202401.0953.v1

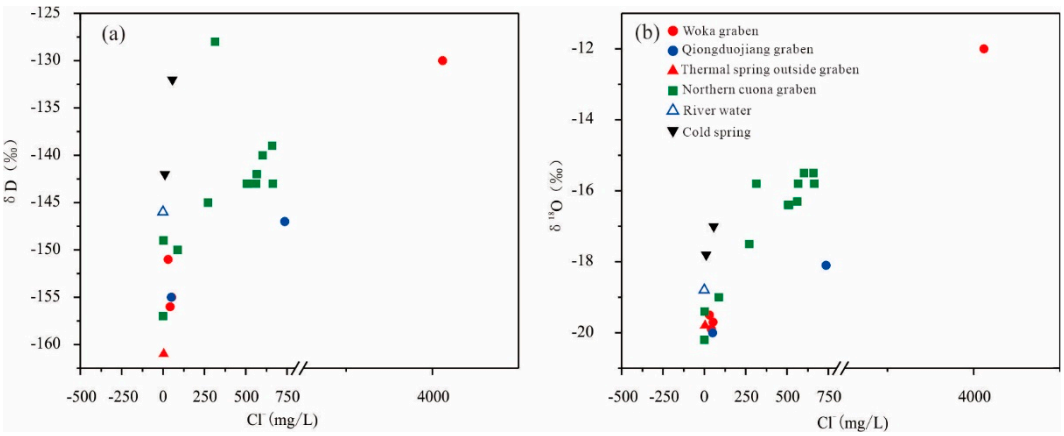

Figure 4. Relationship between δD and Cl- (**a**), δ18O and Cl- (**b**) at sampling points.

The hydrogen and oxygen isotopic characteristics of groundwater recharged by meteoric water exhibit a significant elevation effect, calculated as follows:

$$H = \frac{\delta_G - \delta_p}{K} + h \quad (4)$$

where H denotes the calculated elevation of the recharge area for a groundwater sampling site; δ_G represents the measured δD value of the groundwater in a sampling site, ‰; δ_P signifies the δD value of local meteoric water, ‰; h means the actual elevation of a sampling site, m; K stands for the height-varying δD value of meteoric water, i.e., the height gradient, ‰/100m. Owing to the monsoon climate of the study area, a warm and wet air current moves along the Yarlung Zangbo River valley and is influenced by the elevation effect (the uplift of the Qinghai-Tibet Plateau). This results in a gradual decrease in δD values of meteoric water, with a decline rate of -0.26‰/100m with altitude [12]. The δD value of meteoric water in this study is -126‰, sourced from the rainwater data of the Lhasa Meteorological Station [10].

The calculation results indicate that the recharge elevation of geothermal water in the study area varies from 4500 m to 6200 m, with an average value of 5400 m. Specifically, the recharge elevation is 5100–5300 m (average: 5200 m) in the Woka graben, 4500–6200 m (average: 5400 m) in the northern Cuona graben, and 5300–5500 m in the Qiongduojiang graben and outside the grabens (Table 2). Furthermore, the calculated recharge elevations of river and cold-spring water exceed their actual altitudes, supporting the notion that rivers and cold springs also received meltwater recharge from higher elevations.

Table 2. Elevation of geothermal water recharge in different zones.

Number	Region Name	Recharge Elevation（m）	Surrounding Peaks
1	Woka graben	5100-5300 m, averaging 5200 m	5200- 5500m
2	Qiongduojiang graben	5300-5500 m	5200- 5700m, with the highest peak at 6635 m (La Xiangbo Qingri Peak)
3	Northern Cuona graben	4500-6200 m, averaging 5450 m	4300~6400m, with the highest peak at 6537 m (Kongbu Gangri Peak)
4	Southern Cuona graben	Not calculated	\

 doi:10.20944/preprints202401.0953.v1

5	Extratherm al-Zhegu	6000m	6635 m (La Xiangbo Qingri Peak)

5.2. Subsurface Retention Time and Occurrence Environment of Geothermal Water

Throughout their migration, water vapor and precipitation may undergo changes in environmental conditions, resulting in an imbalance in the fractionation of gas- and liquid-phase isotopes. This leads to varying degrees of deviation between meteoric water lines of different regions and the global meteoric water line in terms of slope and intercept [13,14]. The $\delta^{18}O$ values of groundwater indicate its retention time in the same aquifer, allowing the *d* values to be employed for investigating water-rock interactions, groundwater dynamics, and surface runoff dynamics [15].

$$d=\delta D-8\times\delta^{18}O \quad (5)$$

The slopes of the δD and $\delta^{18}O$ fitted lines of geothermal water in the Woka and northern Cuona grabens are 3.28 (R^2= 0.93; P<0.01) and 3.46 (R^2=0.65; P<0.01), respectively, showcasing typical geothermal water characteristics [16]. To analyze the deuterium excess parameter (*d* value) of geothermal water in the study area, the global meteoric water equation (*d*=10‰) and the characteristics corresponding to d equaling to -40‰, -30‰, -20‰, 0‰, 10‰, and 20‰ were plotted. This facilitated the derivation of the $\delta^{18}O$-δD relationships of geothermal, cold-spring, and river water (Figure 5).

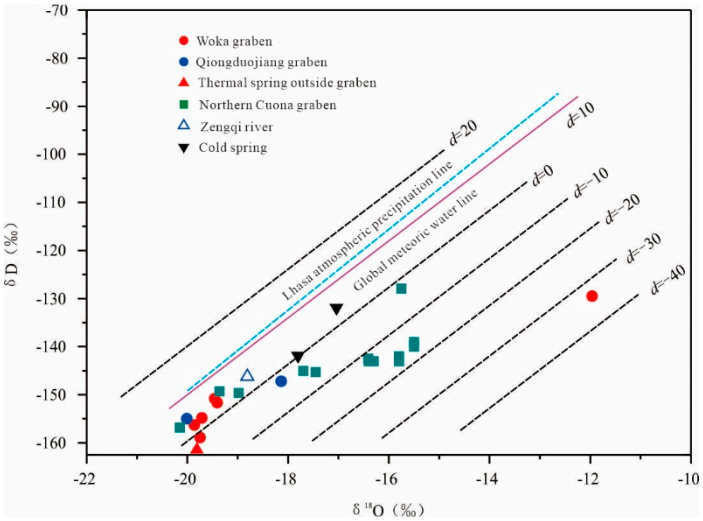

Figure 5. Distribution of d-values at sampling points.

The *d* values of geothermal water from the Woka and northern Cuona grabens ranged from -0.86‰ to 4.88‰ (average: 2.63‰) and -16.6‰–5.58‰ (average: -7.51‰), respectively, confirming a longer subsurface retention time for geothermal water in the northern Cuona graben. Besides the retention time of groundwater in aquifers, the groundwater occurrence environment, such as temperature, also significantly influences the $\delta^{18}O$ values of geothermal water. At low temperatures (<60℃), the lagging isotope exchange between water and rock makes achieving isotopic equilibrium challenging, resulting in non-significant effects on $\delta^{18}O$ values. Conversely, at high temperatures (>80℃), groundwater can absorb energy from the surrounding environment during the runoff process. This leads to the destruction of hydrogen and oxygen atomic bonds inside water molecules, accelerating isotope exchange, causing increased $\delta^{18}O$ values (oxygen drift), and reduced *d* values [17]. The *d* values of cold-spring and river water samples were between 0.5‰ and 4.42‰, indicating the influence of evaporation.

5.3. Carbon Sources of Groundwater

Dissolved inorganic carbon in groundwater primarily originates from atmospheric CO_2, soil CO_2 (mainly from root respiration, microbial activity, and organic matter decomposition), and carbonate

 doi:10.20944/preprints202401.0953.v1

rocks [18]. In active fault zones, geothermal water has a unique carbon source - mantle-derived CO_2 - compared to ordinary cold groundwater [19]. The $\delta^{13}C$ values of atmospheric CO_2, soil CO_2, carbonate rocks, and mantle-derived CO_2 are approximately -7‰, -25‰ (within a range of -16‰–-28‰), -3‰–3‰, and -11‰–-4‰, respectively [20].

The calculated partial pressure of carbon dioxide ($\log pCO_2$) for geothermal water samples in the study area ranged from -4.5 to 0, with an average value of -2.4 (Figure 6a). The global atmospheric $\log pCO_2$ is approximately -3.4, while the high-altitude Qinghai-Tibet Plateau should have a lower $\log pCO_2$ value (<-3.4). Therefore, it is likely that most of the geothermal water in the study area underwent degassing after flowing out of the ground, suggesting minimal influence from atmospheric CO_2. The $\delta^{13}C$ values of geothermal water ranged from -7.3‰ to 2.5‰, averaging -2.5‰, which significantly deviated from the -25‰ of soil CO_2, indicating negligible influence from soil CO_2. The weak correlation between $\delta^{13}C$ and HCO_3^- in geothermal water (Figure 6b) implies that the carbon in geothermal water is not solely derived from metamorphic carbon in carbonate rocks [21]. Considering the hydrogeological and geological conditions of geothermal water exposed in various locations, it is hypothesized that metamorphic carbon in carbonate rocks and mantle-derived CO_2 are two carbon sources for geothermal water in the study area.

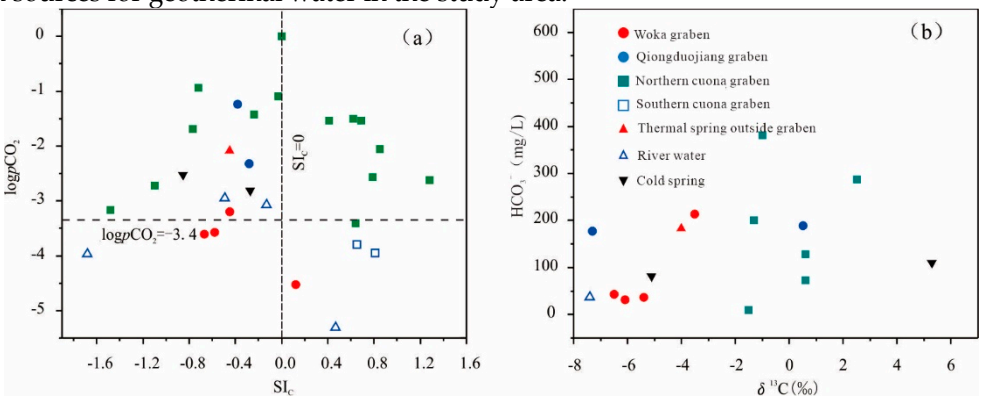

Figure 6. Relationship between SIc-logpCO_2 (**a**) and δ13C-HCO^{3-} (**b**) at sampling points.

The proportions of the two sources of geothermal water can be approximately determined using the law of conservation of isotope mass (Equation. 6).

$$\delta^{13}C_{test}=f\times\delta^{13}C_{metamorphic}+(1-f)\delta^{13}C_{mantle} \quad (6)$$

where $\delta^{13}C_{test}$ denotes the actual test value of $\delta^{13}C$ in geothermal water at a sampling site; $\delta^{13}C_{metamorphic}$ represents the $\delta^{13}C$ value of carbonate rocks; $\delta^{13}C_{mantle}$ signifies the $\delta^{13}C$ value of mantle-derived CO_2; f indicates the proportion of carbonate rock-derived metamorphic carbon in geothermal water, and 1-f means the proportion of carbon from mantle-derived CO_2 in geothermal water. As the $\delta^{13}C$ values of carbonate rocks and mantle-derived CO_2 in the study area were not analyzed, the $\delta^{13}C_{metamorphic}$ and $\delta^{13}C_{mantle}$ values were assumed as 3‰ and -7.5‰, respectively, based on regional characteristics and previous findings [20].

Table 3 presents the following results of the calculation. In geothermal water samples from the Woka graben, the carbon predominantly originated from mantle-derived CO_2, constituting 61%–90% and averaging 80%. The geothermal water from two sampling sites in the Qiongduojiang graben exhibited distinct carbon sources, with mantle-derived CO_2 accounting for 98% in Sewu and only 24% in Qiuduojiang, indicating differing carbon origins for the two sites. Geothermal water samples from the northern Cuona graben showed 5%–42% (average: 29%) of mantle-derived CO_2 and 58%–95% (average: 71%) of metamorphic carbon from carbonate rocks, suggesting the latter as the predominant carbon source. Additionally, geothermal water from Zhegu outside the grabens was predominantly composed of mantle-derived CO_2, constituting 67%.

 doi:10.20944/preprints202401.0953.v1

Table 3. $\delta^{13}C$ values, proportions of metamorphic carbon, and mantle-derived carbon.

Location	Thermal Spring	SI_C	SI_D	SI_G	log(pCO_2)	$\delta^{13}C$	Metamorphic carbon proportion	Mantle-derived carbon proportion
Woka graben	Kanai	-0.67	-3.27	-2.41	-3.61	-6.1	13%	87%
	Woka	-0.58	-2.73	-2.32	-3.57	-6.5	10%	90%
	Cuoba	-0.45	-2.04	-2.17	-3.20	-5.4	20%	80%
	Sangzhuling	0.12	-0.40	-3.35	-4.53	/	/	
Qiongduojiang graben	Sewu	-0.28	-1.20	-3.59	-2.32	-7.3	2%	98%
	Qiongduojiang	-0.24	-0.97	-1.28	-1.43	0.5	76%	24%
Northern Cuona graben	Riruo	-1.10	-2.82	-1.53	-2.72		71%	29%
	Gudui Q004	0.41	0.84	-1.79	-1.54	-1.0	62%	38%
	Gudui Q005	0.64	1.49	-2.09	-3.41	/	/	/
	Gudui Q006	0.79	1.86	-2.23	-2.57	/	/	/
	Gudui Q007	0.62	1.25	-1.80	-1.50	/	/	/
	Gudui H008	1.28	2.30	-1.63	-2.62	/	/	/
	Gudui Q010	0.69	1.34	-1.65	-1.54	/	/	/
	Gudui ZK251	0.00	0.00	0.00	0.00	/	/	/
	Neizongcuo	-1.48	-3.36	-1.75	-3.16	-1.5	58%	42%
	Geimu	-0.77	-1.71	-2.08	-1.69	0.6	77%	23%
	Mulu	-0.03	-0.48	-1.35	-1.09	2.5	95%	5%
	Shuxin	-0.72	-1.93	-1.27	-0.94	-1.3	60%	40%
	Quzhuomu	0.85	0.69	-0.59	-2.06	0.6	77%	23%
Southern Cuona graben	Cuona spring	0.65	0.55	-2.24	-3.79	/	/	/
	Cuona-Drilling	0.81	0.79	-2.46	-3.95	/	/	/
Geothermal water outside the grabens	Zhegu	-0.45	-1.42	-3.13	-2.09	-4.0	33%	67%
River	Zengqi river	0.47	-0.05	-3.60	-5.31	-7.4	/	/
	Jiaboxiong river	-0.13	-0.99	-3.21	-3.08	/	/	/
	Qiena river	-1.68	-99.99	-4.97	-3.97	/	/	/
	Cuona river	-0.49	-1.89	-2.63	-2.95	/	/	/

5.4. Migration Pathways Indicated by Carbon Isotopes in Geothermal Water

In regions characterized by active crustal movements, such as those affected by volcanoes and earthquakes, CO_2 originating from the deep Earth can be released to the surface through deep-seated fault zones. This results in geothermal water along active fault zones being enriched with mantle-derived CO_2 [22]. The hydrothermal activity in Tibet is a consequence of the collisional orogeny between the Eurasian and the Indosinian plates, leading to geothermal fluids in the gas-liquid phase containing valuable information about the upper crust and mantle materials [23]. Geothermal water samples from the Woka graben, Sewu within the Qiongduojiang graben, and Zhegu outside the grabens were predominantly influenced by mantle-derived CO_2. This suggests the presence of deep-seated fault zones serving as ascending pathways for mantle-derived CO_2, indicating high connectivity between the crust and mantle. In contrast, geothermal water samples from the northern Cuona graben and Qiuduojiang within the Qiongduojiang graben displayed relatively high proportions of metamorphic carbon from carbonate rocks. Analyzing calcite, dolomite, and gypsum saturation indices, average values calculated from geothermal water samples of the Woka graben

 doi:10.20944/preprints202401.0953.v1

were -0.39, -1.99, and -2.43, respectively. These values suggest active water-rock interactions and a smooth flow of geothermal water in the Woka graben. Conversely, geothermal water samples from Gudui and Quzhuomu within the northern Cuona graben indicated calcite and dolomite saturation indices above 0, suggesting delayed water-rock interactions. In such cases, when geothermal water reaches the surface, mineral precipitation occurs due to rapid CO_2 degassing, aligning with the sinter sedimentation at spring orifices. Furthermore, the boundary fault F5 in the northern portion of the Gudui geothermal field is an N-dipping high-angle normal fault. Along this fault, a set of carbonate rock interlayers is exposed, with thicknesses ranging from 50 to 100 m and an E-W extension of nearly 30 km. During the ascent of geothermal water along the fault, it may dissolve some carbonate rocks in the runoff process, contributing to an increase in the calcite and dolomite saturation indices.

6. Conclusions

(1) The study area is divided into four zones, each exhibiting distinct hydrochemical characteristics in their geothermal water systems. Geothermal water in the Woka graben is characterized by dominant Na^+ and SO_4^{2-} ions, indicative of a high-temperature system. Similarly, the southern portion of the Qiongduojiang graben displays geothermal water with Na^+ as the dominant cation, resembling that of the Woka graben. Geothermal water in the northern Cuona graben features the highest temperatures and TDS content, along with unusually high Na^+, K^+, and Cl^- values, suggesting a high-temperature geothermal system influenced by deep magmatic activity.

(2) δD and $\delta^{18}O$ values of geothermal water point to its primary origin from meltwater at higher elevations. Analysis of recharge elevation indicates that grabens predominantly receive meteoric water or meltwater from the surrounding mountains. The discernible difference in d values between geothermal water in the Woka and northern Cuona grabens suggests an extended subsurface retention time for the latter.

(3) $\delta^{13}C$ values highlight diverse carbon sources. In the northern Cuona graben, carbon primarily originates from metamorphic carbon in carbonate rocks. Conversely, in other zones, the carbon in geothermal water is predominantly derived from mantle-derived CO_2.

Author Contributions: Conceptualization, W.Z., J.P. and Y.L.; methodology, J.P and Y.L.; software, W.Z.; validation, W.Z., Y.L. and J.P.; formal analysis, W.Z. and Y.L; investigation, W.Z., J.P. and Y.L.; resources, W.Z.; data curation, Y.L. and J.P.; writing—original draft preparation, W.Z.; writing—review and editing, J.P.; visualization, W.Z.; supervision, Y.L.; project administration, W.Z. All authors have read and agreed to the published version of the manuscript.

Funding: This research was funded by the scientific research project entitled Research and Demonstration of Geological Disaster Prevention and Control Technologies for Tibet Autonomous Region initiated by the Department of Natural Resources of Tibet Autonomous Region (Grant No. [2020] 0890-1).

Data Availability Statement: Not available.

Acknowledgments: The authors wish to express their thanks to the director of the Department of Natural Resources of Tibet Autonomous Region, for his valuable assistance.

Conflicts of Interest: The authors declare no conflict of interest.

References

1. Chen, M.X.; Wang, J.Y.; Deng, X. Geothermal system type map and brief explanation in China. *Geological Science* **1996**, 2, 114-121.
2. Wang, G.L.; Zhang, W.; Liang, J.Y.; et al. Evaluation of geothermal resource potential in China. *Acta Geologica Sinica* **2017**, 4, 449-450, 134, 451-459.
3. Yang, B.; Li, W.; Xiong, J.; et al. Health Risk Assessment of Heavy Metals in Soil of Lalu Wetland Based on Monte Carlo Simulation and ACPS-MLR. *Water* **2023**, 15(24), 4223.
4. White, D. Hydrology, activity, and heat flow of the Steamboat Springs thermal system, Washoe County, Nevada. Center for Integrated Data Analytics, Wisconsin, 1968; pp.1-116.
5. Gu, W.Z.; Pang, Z.H.; Wang, Q.J.; et al. *Isotope Hydrology*. Science Press: Beijing, 2011.

6. Li, H.; Liu, M.; Jiao, T.; et al. Using Clustering, Geochemical Modeling, and a Decision Tree for the Hydrogeochemical Characterization of Groundwater in an In Situ Leaching Uranium Deposit in Bayan-Uul, Northern China. *Water* **2023**, 15(24), 4234.
7. Sultan, K.; Faraj, T.; Zaman, Q. Ferric Oxyhydroxylsulfate Precipitation Improves Water Quality in an Acid Mining Lake: A Hydrogeochemical Investigation. *Water* **2023**, 15(24), 4273.
8. Craig, H. Standards for reporting concentrations of deuterium and oxygen-18 in natural waters. *Science* **1961**, 133, 1833–1834.
9. Zheng, S.H.; Hou, F.G.; Ni, B.L. Hydrogen and oxygen stable isotopes in precipitation in China. *Chinese Science Bulletin* **1983**, 13, 801-806.
10. Ning, A.F.; Yin, G.; Liu, T.C. Distribution characteristics of atmospheric precipitation isotopes in the Lhasa River region. *Acta Mineralogica Sinica* **2000**, 20(3), 95-99.
11. Zheng, S.H.; Zhang, Z.F.; Ni, B.L.; et al. Hydrogen and oxygen stable isotope study of geothermal waters in Tibet. *Acta Scientiarum Naturalium Universitatis Pekinensis* **1982**, 1, 99-106.
12. Liu, Z.F.; Tian, L.D.; Yao, T.D.; et al. Temporal and spatial variations of δ18O in precipitation in the Yarlung Zangbo River basin. *Acta Geographica Sinica* **2007**, 62(5), 510-517.
13. Torres-Martínez, J.A.; Mora, A.; Knappett, P.S.K.; et al. Tracking nitrate and sulfate sources in groundwater of an urbanized valley using a multi-tracer approach combined with a Bayesian isotope mixing model. *Water Research* **2020**, 182, 115962.
14. Zhang, J.; Genty, D.; Sirieix, C.; et al. Quantitative assessments of moisture sources and temperature governing rainfall δ18O from 20 years' monitoring records in SW-France: Importance for isotopic-based climate reconstructions. *Journal of Hydrology* **2021**, 591, 125327.
15. Yin, G.; Ni, S.J.; Zhang, Q.C. Deuterium excess parameter and its hydrogeological significance - A case study of Jiuzhaigou and Yele in Sichuan. *Journal of Chengdu University of Technology* **2001**, 28(3), 251-254.
16. Wang, S.Q. Hydrogeochemical processes and formation mechanisms of high-temperature geothermal systems in Tibet. China University of Geosciences (Beijing), 2017.
17. Xiao, K.; Shen, L.C.; Wang, P. Hydrogen and oxygen isotopes of lakes and geothermal waters in the arid region of southern Tibet. *Environmental Science* **2014**, 35(8), 2952-2958.
18. Ren, K.; Pan, X.D.; Zeng, J.; et al. Carbon isotope geochemical characteristics of groundwater under different land uses in karst areas and their ecological significance. *Environmental Science* **2019**, 40(10), 4523-4531.
19. Shangguan, Z.G.; Gao, S.J. Carbon isotope seismogeochemical characteristics of hot springs in the Dianxi experimental field. *Earthquake* **1987**, (06), 27-37.
20. Liu, Z.H.; Yuan, D.X.; He, S.Y.; et al. Geochemical characteristics of the geothermal CO2-water-carbonate rock system and its CO_2 sources - A case study of Huanglonggou Kangding in Sichuan and Xiagei in Yunnan. *Science in China (Series D)* **2000**, 30(002), 209-214.
21. Zhang, Y.H. Genesis and exploitation of the Kangding-Moxi segment of the Xianyu River fault geothermal system. Chengdu University of Technology, 2018.
22. Frondini, F.; Caliro, S.; Cardellini, C.; et al. Carbon dioxide degassing and thermal energy release in the Monte Amiata volcanic-geothermal area (Italy). *Applied Geochemistry* **2009**, 24(5), 860-875.
23. Shen, L.C.; Wu, K.Y.; Xiao, Q.; et al. CO_2 degassing in the geothermal anomaly area of Tibet: A case study of Langju and Dagejia geothermal areas. *Chinese Science Bulletin* **2011**, 56(26), 2198-2208.